

Cell Reports, Volume 37

Supplemental information

Anti-recombination function of MutS α

restricts telomere extension

by ALT-associated homology-directed repair

**Jonathan Barroso-González, Laura García-Expósito, Pablo Galaviz, Michelle Lee
Lynskey, Joshua A.M. Allen, SongMy Hoang, Simon C. Watkins, Hilda A.
Pickett, and Roderick J. O'Sullivan**

Figure. S1.

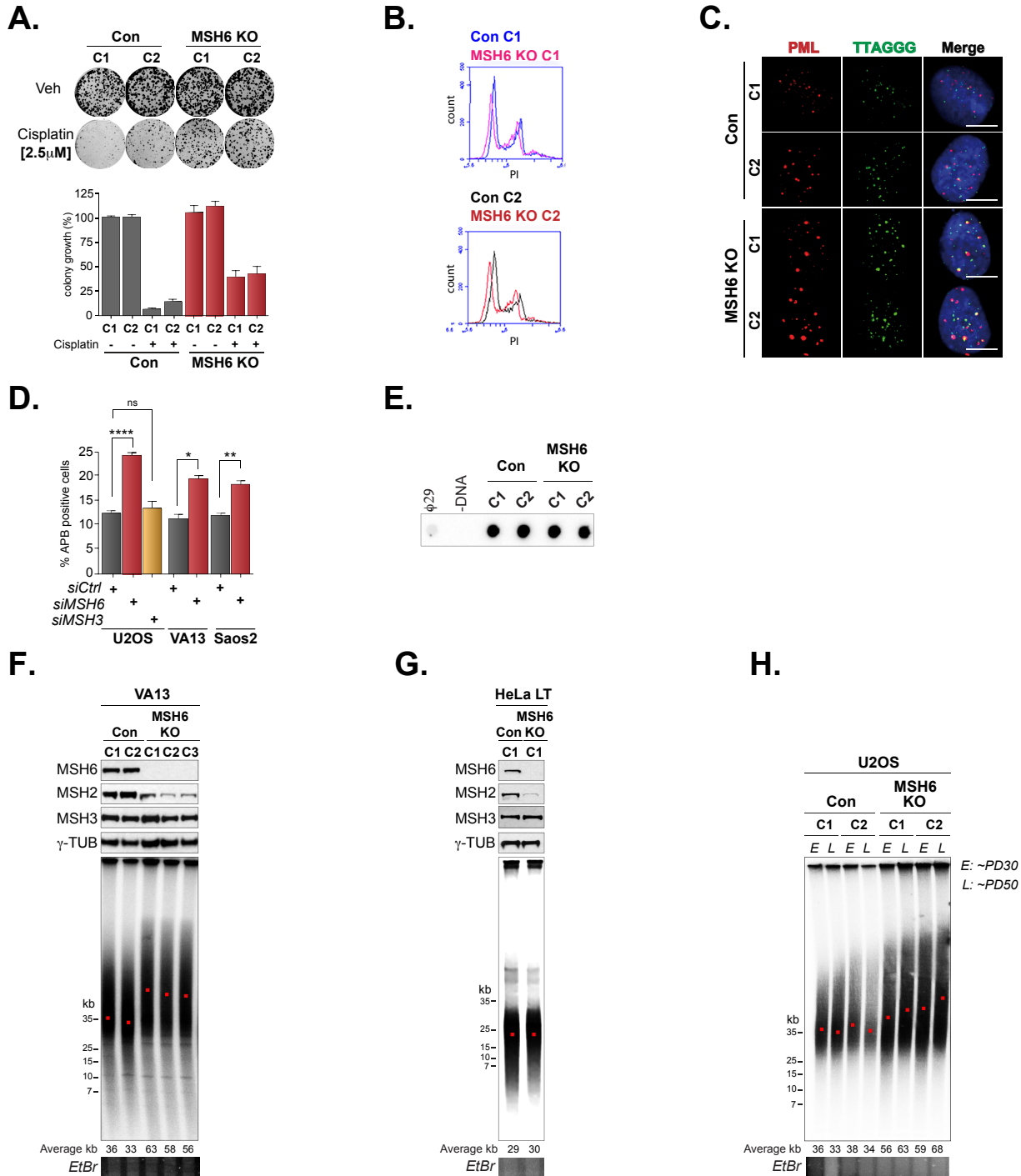


Figure S1. Related to Figure 1. MutS α regulates telomere maintenance in ALT cells. (A) Images and quantification of colony formation assays with U2OS control and MSH6 KO clones treated with vehicle or 2.5 μM cisplatin. (B) Profiles of cell cycle phasing in proliferating U2OS control and MSH6 KO clones. (C) Representative IF-FISH images of ALT-associated PML Bodies (APBs) in U2OS control and MSH6 KO clones. (D) Quantification of APBs by IF-FISH in U2OS, Saos2, and VA13 (ALT positive) cells after siRNA mediated depletion of MSH6 or MSH3. (E) Representative image of Southern blot detection of C-circles in U2OS control and MSH6 KO clones. (F) Top: Western Blot showing MSH6 depletion in VA13 cells (ALT+) by CRISPR/Cas9. γ-Tubulin is shown as a loading control. Bottom: Telomere length analysis of control (C1 and C2) and MSH6 KO (C1, C2, and C3) clones after 25 population doubling (PD) by pulsed field gel electrophoresis (PFGE). Telomere size (kb) is shown below, and ethidium bromide (EtBr) image is used as a loading control for PFGE. Red dot indicates average TRF length. (G) Top: Western Blot showing MSH6 depletion in HeLa LT cells (telomerase positive) by CRISPR/Cas9. γ-Tubulin is shown as a loading control. Bottom: Telomere length analysis of control (C1) and MSH6 KO (C1) clones after 25 PD by PFGE. Telomere size (kb) is shown below, and ethidium bromide (EtBr) image is used as a loading control. Red dot indicates average telomere length. (H) Telomere length analysis of U2OS control and MSH6 KO clones after 30 PD and 50 PD by PFGE. Ethidium bromide (EtBr) image is used as a loading control. All data represent mean ± SEM, n=3 biological replicates. *p < 0.05, **p < 0.01, ***p < 0.0001 (One way ANOVA). Unless otherwise indicated, all FISH experiments were conducted using TelC FISH probe. All scale bars, 5 μm.

Figure. S2.

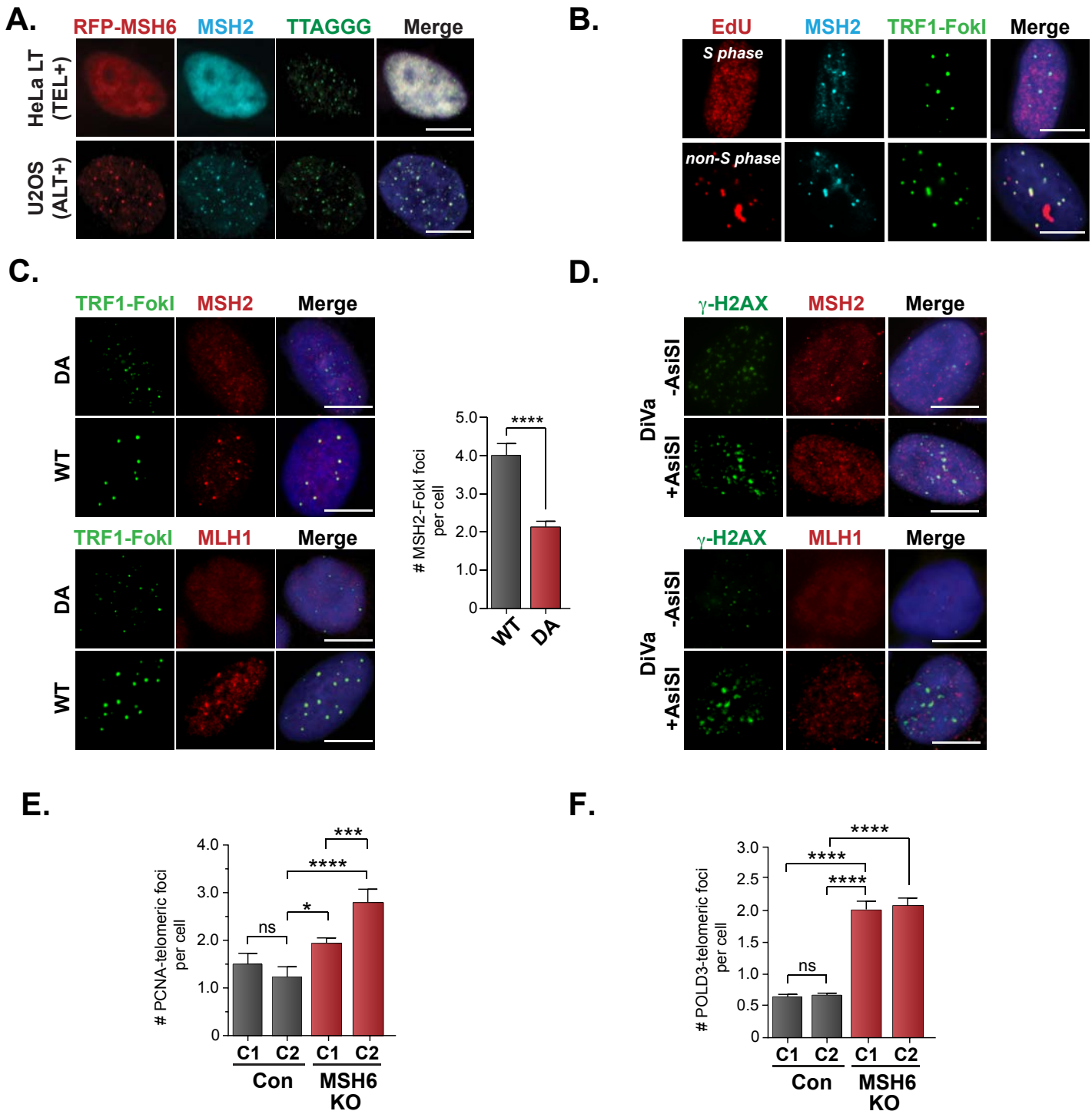
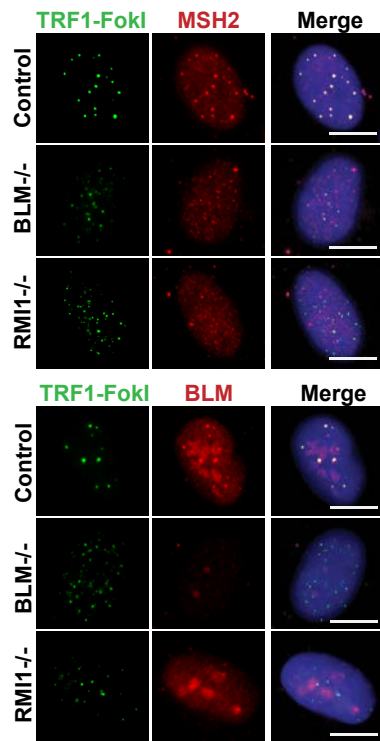


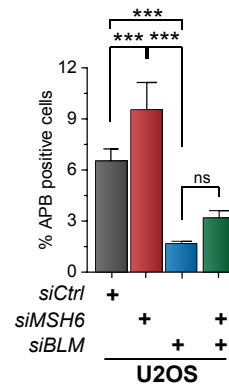
Figure S2. Related to Figure 2. Specific recruitment of MutS α to telomere DNA breaks. (A) Representative IF-FISH images of endogenous MSH2 and RFP-MSH6 co-localization with telomeres in HeLa LT (telomerase positive) and U2OS (ALT positive) cancer cells. (B) Representative IF images of endogenous MSH2 and EdU co-localization with TRF1-FokI induced DSBs. (C) Representative IF images of MSH2 or MLH1 colocalization to wildtype (WT) and inactive (DA)-TRF1-FokI telomere double strand breaks. Quantifications are placed adjacent. (D) Representative IF images of MSH2 or MLH1 colocalization with γ -H2AX at sites of AsiSI-induced double strand breaks in U2OS DiVa cells. (E) Quantification of PCNA and (F) POLD3 telomeric foci in control and MSH6 KO U2OS clones. All data represent mean \pm SEM, $n=3$ biological replicates, except C, $n=2$. *** $p < 0.001$, (One way ANOVA). Unless otherwise indicated, all FISH experiments were conducted using TelC FISH probe. All scale bars, 5 μ m.

Figure. S3.

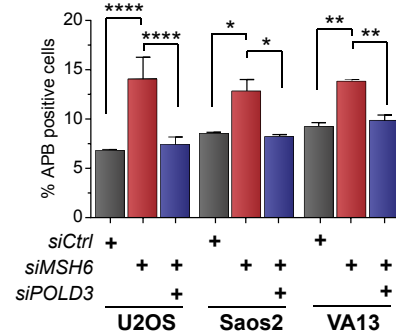
A.



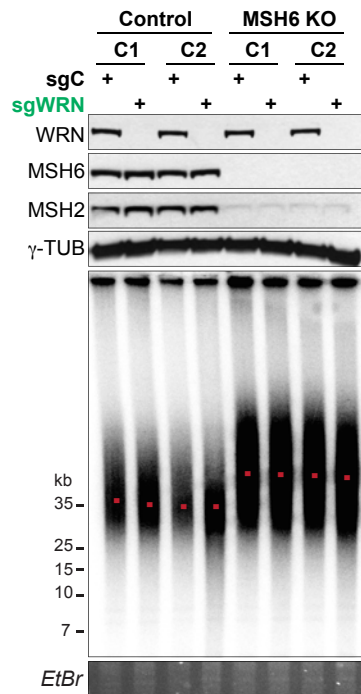
B.



C.



D.



E.

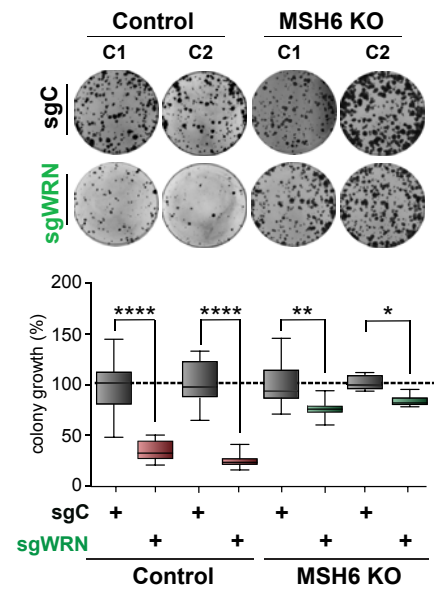
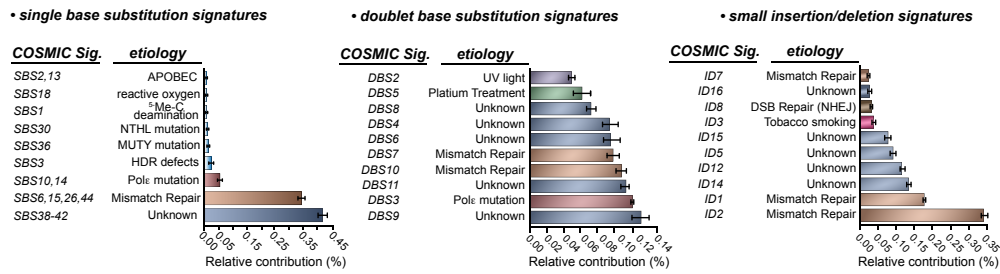


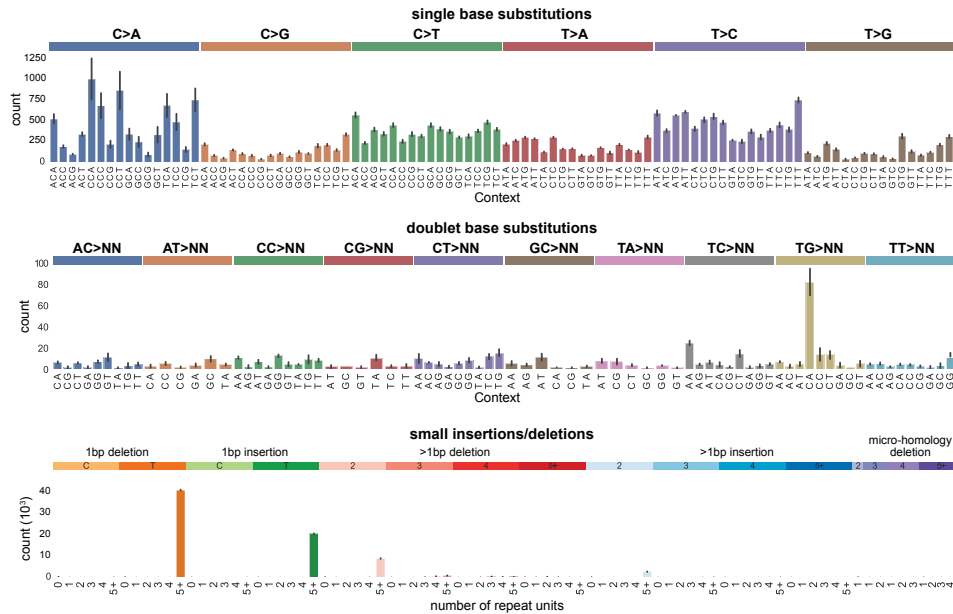
Figure S3. Related top Figure 3. Regulation of MutS α by BLM helicase and POLD3, but not WRN helicase. (A) Representative IF images showing colocalization of MSH2 or BLM to TRF1-FokI telomeres in BLM or RMI depleted U2OS control and MSH6 KO clones. **(B)** Analysis of APBs in U2OS cells with MSH6 or BLM siRNA knockdown. **(C)** Analysis of APBs in U2OS, Saos2, and VA13 cells with MSH6 or POLD3 siRNA knockdown. **(D)** Top: Western blot of WRN depletion in U2OS control and MSH6 KO clones by CRISPR/Cas9. γ -Tubulin is shown as a loading control. Bottom: Telomere length analysis of WRN deficient U2OS control and MSH6 KO clones by PFGE. EtBr gel is used as a DNA loading control. **(E)** Images (left) and quantifications (right) of colony formation assays with WRN deficient U2OS control and MSH6 KO clones. All pairs are quantified relative to their respective control clone. All data represent mean \pm SEM, n=3 biological replicates. *p < 0.05, **p < 0.01, ***p < 0.001, ****p < 0.0001 (One way ANOVA). Unless otherwise indicated, all FISH experiments were conducted using TelC FISH probe. All scale bars, 5 μ m.

Figure. S4.

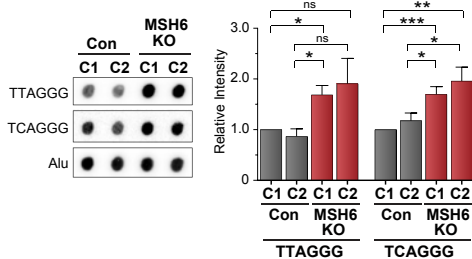
A.



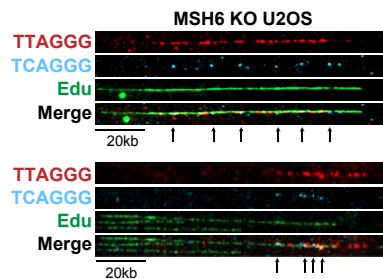
B.



C.



D.



E.

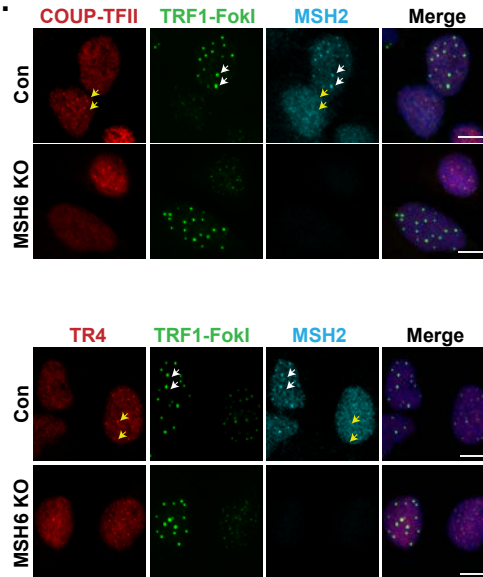
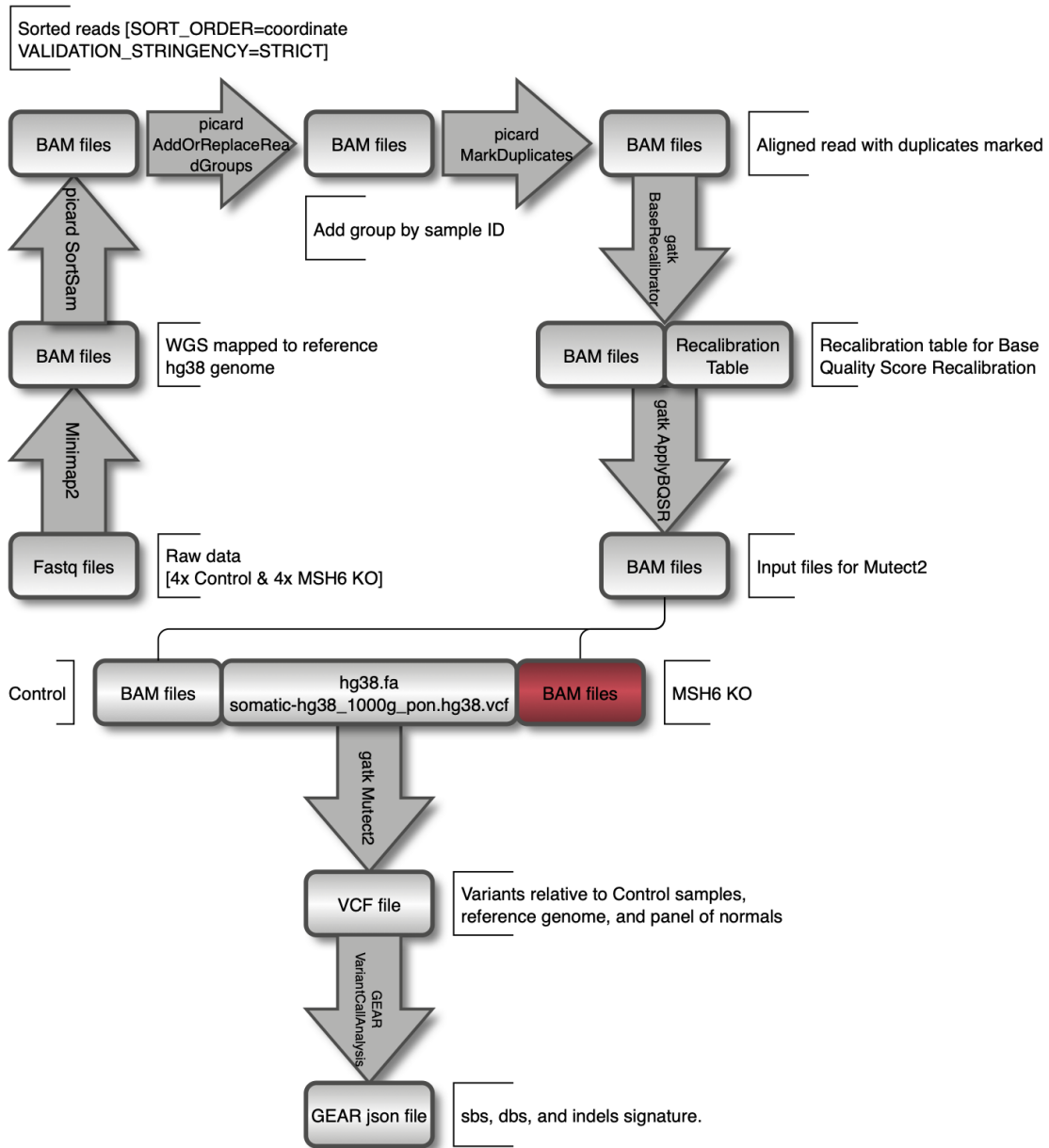


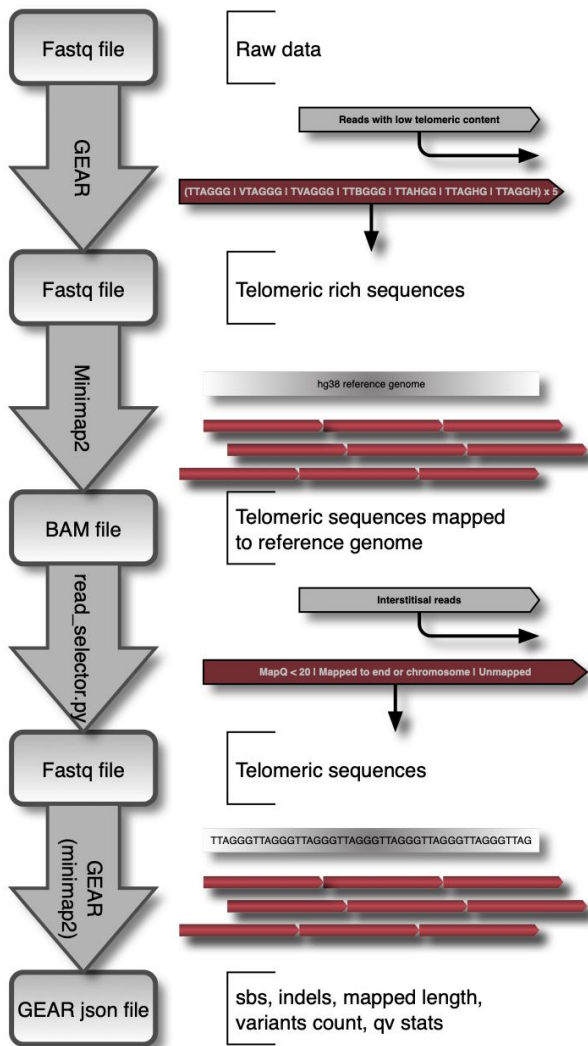
Figure S4. Related to Figure 4. Genome-wide mutational signatures and telomere variant repeat analyses in MutS α deficient ALT cancer cells. (A) The frequency of all COSMIC single base substitution (SBS), doublet base substitutions (DBS) and small insertion/deletion (ID) signatures identified in MSH6 KO clones (C1 and C2), that were not present in controls, and their respective etiological contribution. Germline mutations are not shown. (B) The contribution and average number of SBS, DBS and small indels (ID) to the mutational signatures identified in MSH6 KO U2OS cells. (C) Left: Dot blots of digested genomic DNA from U2OS control and MSH6 KO cells probed with either TCAGGG or TTAGGG probes. The ALU probe was used for total DNA loading control. Right: Relative quantification of TCAGGG and TTAGGG dot blot signals normalized to ALU control in control and MSH6 KO clones. (D) DNA fiber analysis by SMAT of telomere extension events in U2OS control and MSH6 KO cells using EduU-positive fibers showing interspersed of TCAGGG at the telomere. (E) Representative IF images of endogenous COUP-TFII and TR4 co-localization with TRF1-FokI and endogenous MSH2 in U2OS control and MSH6 KO cells. White arrows indicate colocalizing MSH2 and TRF1-FokI DSB sites. Yellow arrows mark sites of COUP-TFII and TR4 accumulation. Data in C represents mean \pm SEM, n=3 biological replicates. *p < 0.05, **p < 0.01, ***p < 0.001, (One way ANOVA). For A-B, 95% confidence interval error bars are shown.

Figure S5. Related to STAR Methods



Method 1. Variant call and mutational signature workflow.

Figure S6. Related to STAR Methods



Method 2. Telomere analysis workflow.